

Photomagnetic effect in the CdCr_2Se_4 ferromagnetic semiconductor

E. Mosiniewicz-Szablewska and H. Szymczak

Institute of Physics, Polish Academy of Sciences, Al. Lotników 32/46, 02-668 Warsaw, Poland

(Received 17 August 1992)

The influence of infrared irradiation on the ferromagnetic resonance (FMR) of CdCr_2Se_4 single crystals has been investigated in the temperature range 4.2–130 K. It was found that the irradiation induced appreciable changes in the microwave conductivity, FMR line shape, FMR linewidth, and magnetocrystalline anisotropy of this material. These findings are discussed by taking into account three different mechanisms: the slow relaxation mechanism, the appearance of low-symmetry fields at the Cr^{2+} Jahn-Teller centers, and the skin effect.

I. INTRODUCTION

The chalcogenide spinel CdCr_2Se_4 is a semiconductor and a single-sublattice ferromagnet with a relatively high Curie temperature $T_c = 130$ K.¹ Its magnetic system is formed by trivalent chromium ions, which can change their valence by doping or deviations in stoichiometry.² The selenium vacancies, which lead to the appearance of Cr^{2+} ions on the octahedral sites, are predominant among the CdCr_2Se_4 structure defects. Donor doping increases the number of Cr^{2+} ions and acceptor doping results in the formation of Cr^{4+} ions.

The photomagnetic properties of CdCr_2Se_4 have been investigated thoroughly for more than 20 years. It has been found that infrared irradiation produced considerable changes in the permeability, magnetization, and coercive force^{3,4} of this material. These phenomena have been interpreted as the result of light-induced electron transitions, resulting in a redistribution of Cr^{2+} ions in the crystal. These transitions correspond to a change in the chromium-ion valence according to the scheme $\text{Cr}^{3+} + e^- \rightarrow \text{Cr}^{2+}$ and are assumed to occur between the valence band and impurity Cr^{2+} levels situated below the bottom of the conduction band.⁴

As the result of the above-mentioned transitions, electrons can localize at the Cr^{2+} levels creating strongly anisotropic centers which may interact with domain walls. The appearance of such a center near the domain wall should lead to both a change in domain-wall thickness and a decrease in domain-wall mobility.

All the above-mentioned photomagnetic effects have been investigated in magnetically nonsaturated samples. In the case of the ferromagnetic resonance (FMR) of CdCr_2Se_4 , which occurs for high magnetic fields in which the sample becomes saturated, the assumption about the interaction between the light-induced Cr^{2+} centers and domain walls makes no sense. Therefore, the photomagnetic changes in the FMR spectra of CdCr_2Se_4 are expected to give a deeper insight into the nature of the photomagnetic centers in comparison with the information obtained from the measurements performed on nonsaturated samples. Preliminary results of this work have been briefly reported.⁵

II. EXPERIMENTAL DETAILS

The single crystals used in the experiment were Ga-doped, Ag-doped, and undoped CdCr_2Se_4 grown by spontaneous crystallization from a melt of pure CdSe and CrCl_3 at the Institute of General Physics of the Academy of Sciences, Moscow, Russia. FMR experiments were performed on a standard X-band spectrometer operating at 9.1 GHz with 100-kHz field modulation. FMR spectra were recorded in a (110) plane before and after irradiation with light in the wide temperature range 4.2–300 K. Spectral dependences of the photomagnetic effect were investigated in the wavelength range 300–2500 nm using a monochromator with a NaCl prism.

III. EXPERIMENTAL RESULTS

Under the influence of light the intensity of the FMR signal decreased and the FMR line became more asymmetrical about the field for resonance. The irradiation with light also induced appreciable changes in the resonance field and FMR linewidth.

The dependence of the FMR signal intensity I on irradiation is shown in Fig. 1. After cooling in the dark to

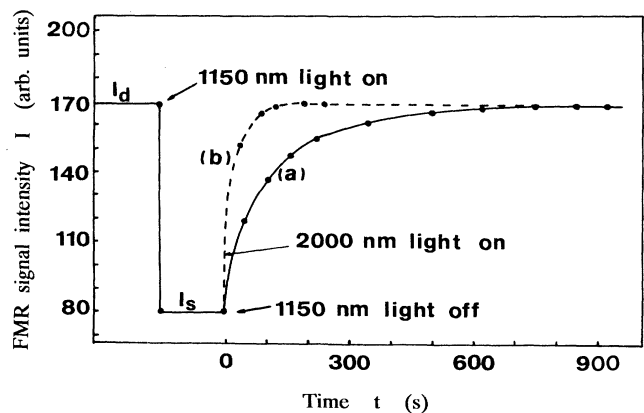


FIG. 1. FMR signal intensity as a function of time. Curve (a), the recovery process after switching off the 1150-nm light. Curve (b), the quenching of the photomagnetic changes after switching on the 2000-nm light.

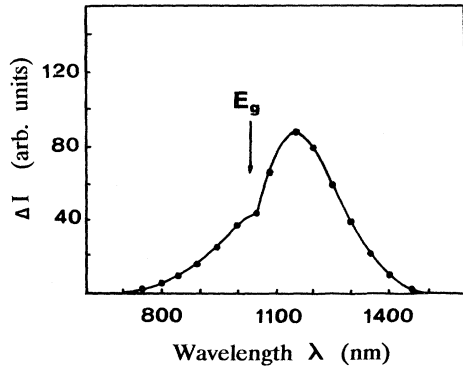


FIG. 2. Change in the FMR signal intensity as a function of wavelength.

4.2 K, an initial intensity I_d was noted. When the light was switched on I decreased rapidly to a much lower stationary value I_s . Afterwards the light was switched off and I returned relatively slowly to its original level I_d [see Fig. 1, curve (a)].

The stationary value I_s , reached after irradiation, was found to depend on the wavelength and intensity of light. Figure 2 shows the change in the intensity of the FMR signal $\Delta I = I_d - I_s$ plotted as a function of wavelength. The photoinduced changes in the FMR spectra of CdCr_2Se_4 were produced by photons with wavelengths in the range 800–1500 nm and reached a maximum at 1150 nm. In Fig. 2, one can also see the second maximum of ΔI at 1070 nm which corresponds to the value of the band-gap energy $E_g = 1.16$ eV. This value is in good agreement with that obtained earlier for CdCr_2Se_4 at 4.2 K.⁶

As could be seen above, when the light was switched off the FMR signal intensity I returned slowly to its initial level I_d [see Fig. 1, curve (a)]. It was also noted that the recovery process proceeded much faster when, at the moment $t=0$, the 2000-nm infrared radiation was switched on [see Fig. 1, curve (b)]. Such a quenching of the photomagnetic effect was found to occur in the wavelength range 1500–2300 nm and it reached a maximum at 1900 nm (see Fig. 3).

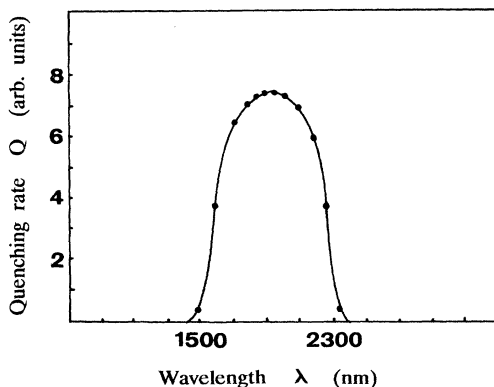


FIG. 3. Quenching rate, defined as $\nu = \Delta I/t$, as a function of wavelength.

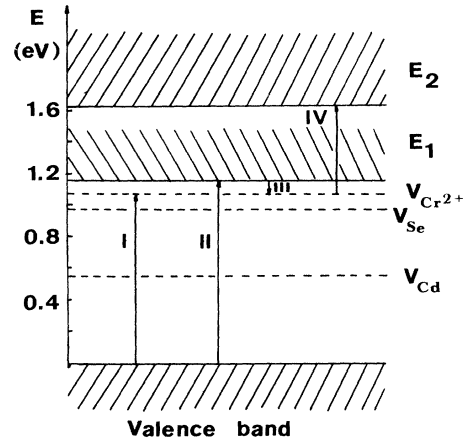


FIG. 4. Schematic CdCr_2Se_4 band structure and transitions corresponding to the photomagnetic changes in the FMR parameters.

The experimental results can be interpreted within the framework of a band model. At the distance of 1.16 eV from the valence band there is a narrow conduction band consisting of $\text{Cr}^{2+}(3d^4)$ electrons^{4,7} (see Fig. 4). The transitions between these two bands correspond to a change in the chromium-ion valence according to the scheme $\text{Cr}^{3+} + e^- \rightarrow \text{Cr}^{2+}$. The observed light-induced changes in the FMR parameters may be caused by photoinduced electron transitions between the valence band and localized Cr^{2+} levels situated at a distance of 0.08 eV below the bottom of the conduction band (see Fig. 4).

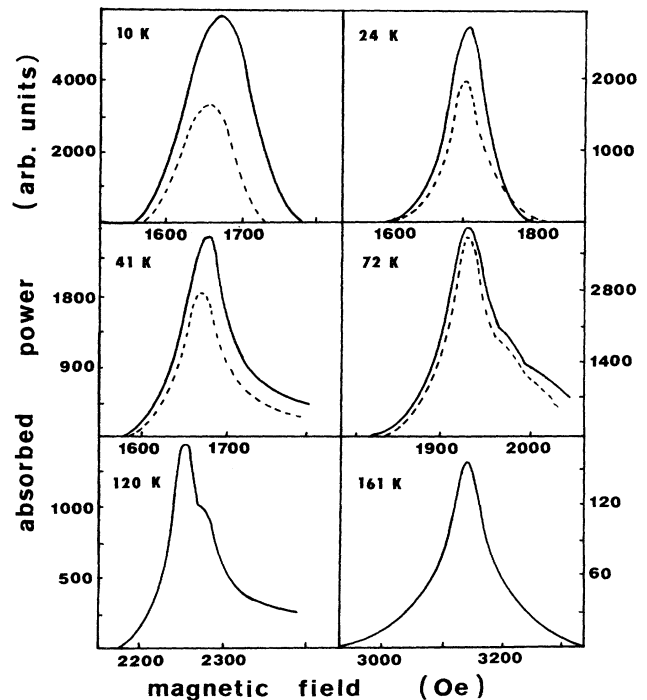


FIG. 5. FMR line shape before (solid curve) and after (dotted curve) irradiation with infrared light for various temperatures.

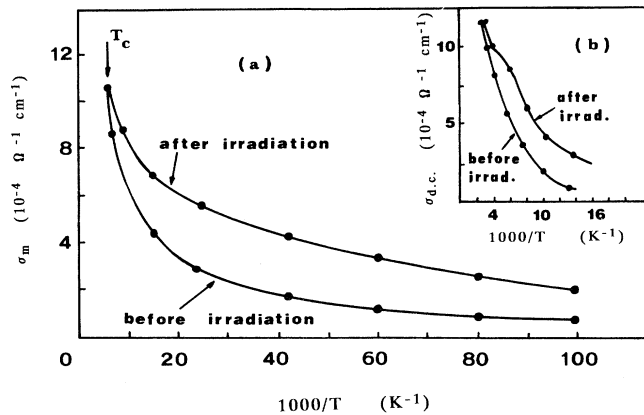


FIG. 6. (a) Microwave conductivity of CdCr_2Se_4 as a function of reciprocal temperature, (b) dc conductivity of CdCr_2Se_4 as a function of reciprocal temperature (Ref. 9).

These transitions may occur either directly (transition I) or indirectly, i.e., through the conduction band (transitions II+III).

The existence of the Cr^{2+} levels may be attributed to lattice deformations caused by vacancies or other point defects (like Ga^{3+} ions). These deformations lead to the appearance of the localized Cr^{2+} levels at the expense of a change in the number of states in the $\text{Cr}^{2+}(3d^4)$ conduction band.^{4,7}

As the result of the above-mentioned transitions, electrons, photoactivated from the valence band, are trapped on the octahedral Cr^{3+} sites creating Cr^{2+} centers. The holes remaining in the valence band contribute to the microwave conductivity of the irradiated samples.

The observed quenching of the photomagnetic effects may be caused by the photoinduced electron transitions between the above-mentioned Cr^{2+} levels and other broad conduction band⁷ from which the recombination process occurs much faster (see transitions IV in Fig. 4).

Figure 5 shows the ferromagnetic resonance spectra before and after irradiation with infrared light for various temperatures. The observed light-induced decrease in the FMR signal intensity and the asymmetrical line shape

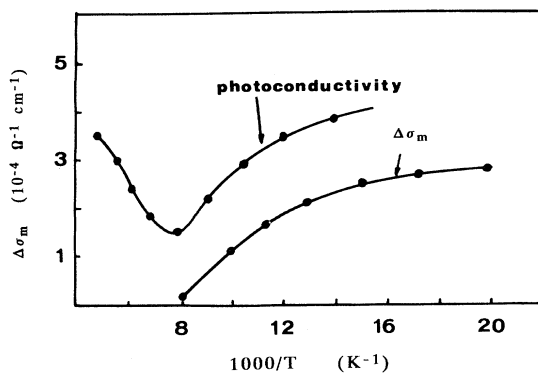


FIG. 7. Change in the microwave conductivity of CdCr_2Se_4 and photoconductivity (Ref. 10) as functions of reciprocal temperature.

may be attributed to the change in skin depth. (The influence of the skin effect on the FMR line shape has been reported earlier for impurity-doped CdCr_2Se_4 .⁸)

The temperature dependence of the microwave conductivity, obtained by means of the FMR spectra presented in Fig. 5, is shown in Fig. 6(a). This temperature dependence is very similar to that of dc conductivity measured earlier for CdCr_2Se_4 (Ref. 9) [see Fig. 6(b)].

It was also noted that the light-induced change in the microwave conductivity $\Delta\sigma_m = \sigma_m^{\text{unirr}} - \sigma_m^{\text{irr}}$ plotted as a function of temperature is similar to the temperature dependence of photoconductivity reported previously for CdCr_2Se_4 (Ref. 10) (see Fig. 7).

As was mentioned above, the intensity of the FMR signal decreases with an increase in the intensity of irradiation [see Fig. 8(a)]. The skin depth δ and microwave conductivity σ_m as functions of the intensity of light, obtained by means of the curve shown in Fig. 8(a), are plotted in Figs. 8(b) and 8(c).

Figure 9 shows the resonance field H_{rez} and FMR linewidth ΔH as functions of the angle between the applied magnetic field and the direction of the easy magnetization [001] in the (110) plane. The salient feature is an increase in the magnetocrystalline anisotropy after illumination, which might be caused by a light-induced increase in the number of Cr^{2+} ions in the crystal. It is also worth noting that after annealing in vacuum and in the selenium atmosphere no photomagnetic changes in the FMR spectra were observed.

The photomagnetic changes in the FMR parameters

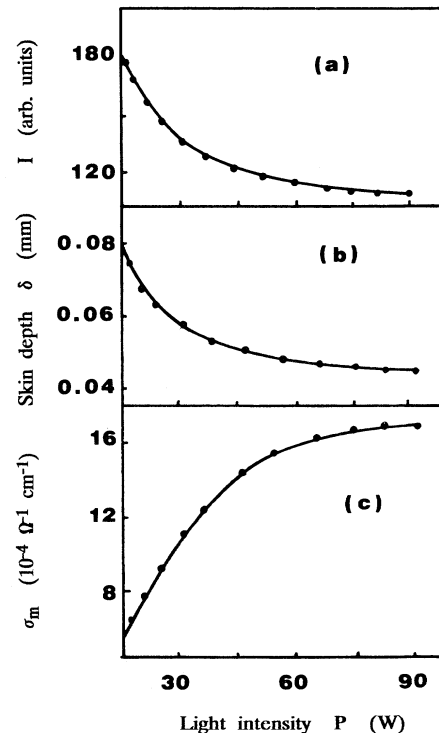


FIG. 8. (a) FMR signal intensity, (b) skin depth, (c) microwave conductivity as functions of the intensity of light.

appeared only below $T_c = 130$ K (see Fig. 10) and increased with a decrease in temperature. It was also found that the photomagnetic effects were stronger for crystals with a higher degree of nonstoichiometry and for Ga-doped samples. For most stoichiometric crystals and for Ag-doped samples no photoinduced changes were observed.

IV. DISCUSSION

The observed temperature and angular dependences of the resonance field and FMR linewidth could be explained by taking into account the following two different mechanisms: (i) the slow relaxation mechanism in which the observed anomalies are attributed to the impurity Cr^{2+} ions with near crossing energy levels in the $[111]$ direction,¹¹ and (ii) the appearance of random low-symmetry fields acting on the Jahn-Teller Cr^{2+} ions on the octahedral sites.¹²

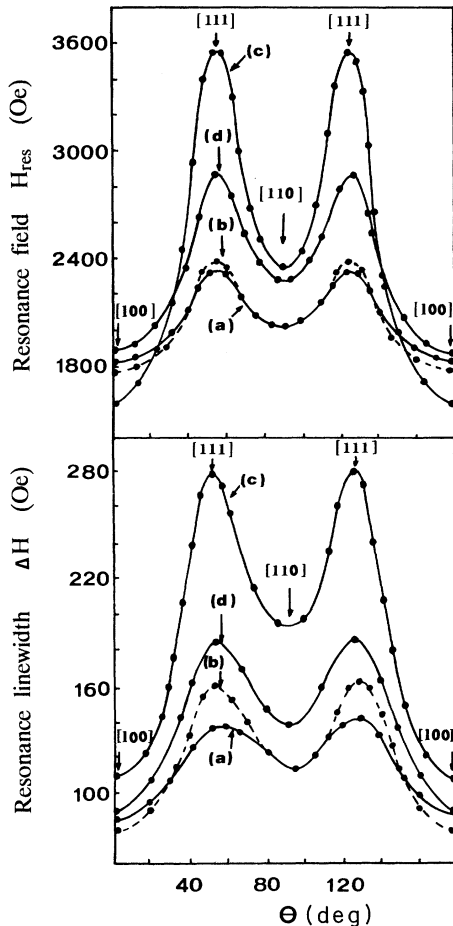


FIG. 9. Resonance field and FMR linewidth as functions of the angle between the applied magnetic field and the direction of the easy magnetization $[001]$ in a (110) plane: (a) before irradiation, (b) after irradiation with the 1150-nm light, (c) after annealing in vacuum, (d) after annealing in the selenium atmosphere. The theoretical curves are calculated by means of Eq. (2) and (3).

The slow relaxation mechanism is responsible for the giant anomalous peaks of H_{rez} and ΔH along the $[111]$ direction due to the presence of the impurity Cr^{2+} ions, which arise on the octahedral sites to compensate the charge for Ga doping or Se vacancies.¹³ As mentioned above, these ions can also be created by light irradiation.

The Cr^{2+} ion has the lowest 5E doublet in the octahedral crystal field. This doublet is split in second order by the spin-orbit coupling and the local crystalline field of trigonal symmetry. The anomalies in the angular and temperature dependences of H_{rez} and ΔH occur as the result of near crossovers of these low-lying energy levels.¹¹

The slow relaxation mechanism has been analyzed earlier by Clogston¹⁴ and Gurevich.¹¹ Before discussing the experimental results, we present some related ideas and cite the few theoretical results we shall need later on.

The system under investigation consists of two subsystems. The first is the ferromagnetically ordered subsystem formed, in our case, by Cr^{3+} ions. The excitations of this subsystem are collective excitations (magnons) and we can describe this subsystem by means of the magnetization vector

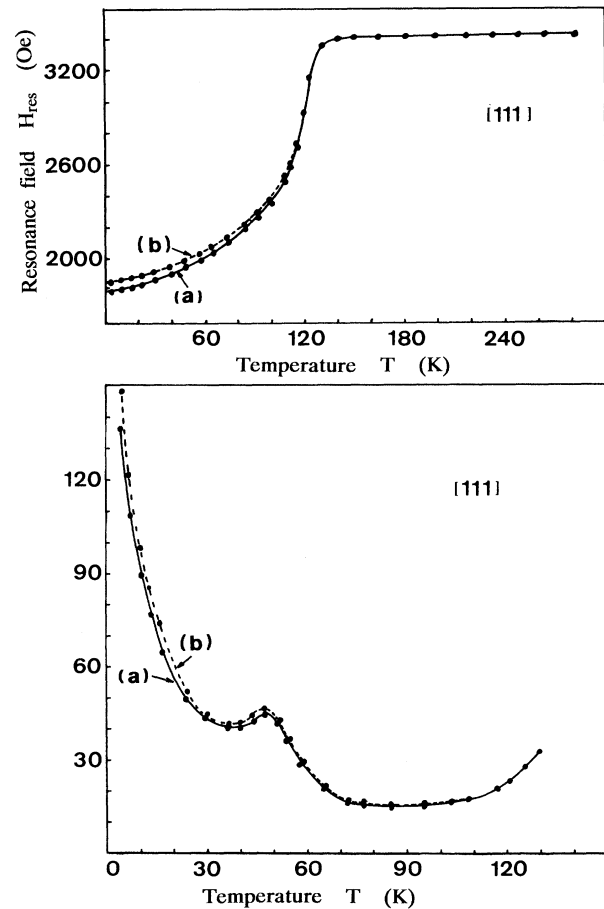


FIG. 10. Temperature dependences of the resonance field and FMR linewidth before [curves (a)] and after [curves (b)] irradiation with the 1150-nm light.

$$\mathbf{M} = \mathbf{M}_0 + \mathbf{m} \exp(i\omega t) \quad (1)$$

that satisfies the Landau-Lifshits equation of motion.

The second subsystem is formed by the impurity ions, in our case, by Cr^{2+} ions. Strong spin-orbit coupling is characteristic of this subsystem. If there are not very many such impurity ions (only this case will be considered) the subsystem can be regarded as consisting of individual paramagnetic ions, noninteracting with each other.

$$\delta H_{\text{rez}} \equiv H_{\text{rez}} - \omega/\gamma$$

$$= \frac{1}{2} N/M_0 \Delta E_{\text{max}} \left\{ \frac{3}{2} \Delta E_{\text{max}}/\Delta E [3 \sin^2\theta + 3 \sin^2 2\theta - 2 - \frac{3}{2} (\Delta E_{\text{max}}/\Delta E)^2 \sin^2 2\theta (1 - \frac{3}{2} \sin^2\theta)^2] \right. \\ \left. \times \tanh(\Delta E/kT) + \frac{9}{4} \Delta E_{\text{max}}/kT \Delta E_{\text{max}}/\Delta E \sin^2 2\theta (1 - \frac{3}{2} \sin^2\theta)^2 \cosh^{-2}(\Delta E/kT) \right\} \quad (2)$$

and

$$2\Delta H = N/M_0 1/kTP \cosh^{-2}(\Delta E/kT) \omega\tau / [1 + (\omega\tau)^2], \quad (3)$$

where

$$\Delta E = \Delta E_{\text{max}} [(1 - \frac{3}{2} \sin^2\theta)^2 + \xi^2]^{1/2},$$

$$\xi = \Delta E_{\text{min}}/\Delta E_{\text{max}},$$

$$P = \frac{9}{4} (\Delta E_{\text{max}})^2 \sin^2 2\theta (1 - \frac{3}{2} \sin^2\theta)^2 / [(1 - \frac{3}{2} \sin^2\theta)^2 + \xi^2],$$

ΔE_{min} and ΔE_{max} are the separations between the low-lying energy levels for the [111] and [001] directions, respectively, and N is the concentration of Cr^{2+} ions in the sample.

The temperature dependence of ΔH , besides the explicit dependence on T in Eq. (3), is determined by the temperature dependence of τ . Then an assumption should be made concerning the temperature dependence of the ion relaxation time τ .

Ion can pass the energy subtracted from the magnetically ordered subsystem not only to the lattice, but also back to the magnetically ordered subsystem, exciting the

The subsystems are coupled by an exchange interaction, that, in general, is anisotropic. It results in strong anisotropy of the ion energy spectrum, i.e., in the dependence of the energy levels on the angles between \mathbf{M} and the crystal axes. In particular, crossings or near crossings of the levels can take place.

The contributions of the impurity paramagnetic ions to the resonance field and FMR linewidth for the (110) plane can be written in the form¹¹

$k \neq 0$ magnons. The corresponding ion relaxation mechanisms have been named spin-phonon and spin-magnon processes. The $\tau(T)$ dependences are the same for these processes. Both above-mentioned processes can be direct, Raman, and Orbach ones. Assuming that in our case the direct processes prevail (as it takes place at low temperatures), we obtain¹¹

$$\tau = \tau_0 \tanh(\Delta E/kT). \quad (4)$$

The $\Delta H(T)$ dependence is characterized now by four parameters ΔE_{min} , ΔE_{max} , N , and τ_0 .

Figures 9 and 11(a) show the fits of $H_{\text{rez}}(\theta)$, $\Delta H(\theta)$, and $\Delta H(T)$ obtained by taking into account Eqs. (2) and (3). By means of these fits one can calculate the separations between the low-lying energy levels of the Cr^{2+} ion for the [001] and [111] directions and the concentrations of Cr^{2+} ions in the samples.

The separations between the energy levels are equal to

$$\Delta E_{\text{max}}/k = 28.7 \pm 0.9 \text{ K for [001] direction,}$$

$$\Delta E_{\text{min}}/k = 11.1 \pm 0.4 \text{ K for [111] directions.}$$

The concentrations of Cr^{2+} ions are equal to

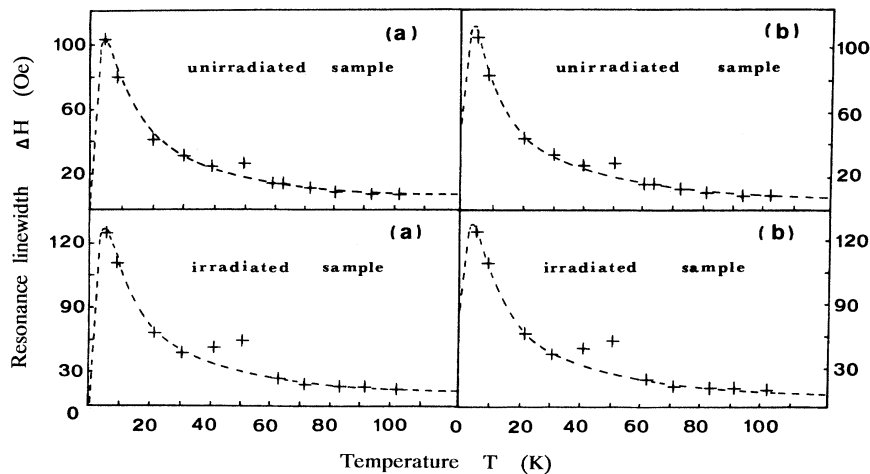


FIG. 11. Experimental temperature dependencies of the FMR linewidth before and after irradiation with the 1150-nm light. The theoretical curves are obtained by taking into account (a) the slow relaxation mechanism [see Eq. (3)] and (b) the Jahn-Teller mechanism [see Eq. (5)].

$N_1 = (1.10 \pm 0.03) \times 10^{19} / \text{cm}^3$ for the unirradiated sample ,

$N_2 = (1.20 \pm 0.04) \times 10^{19} / \text{cm}^3$ for the sample irradiated with the 1150-nm light of intensity $P = 90 \text{ W}$,

$N_3 = (4.00 \pm 0.12) \times 10^{19} / \text{cm}^3$ for the sample annealed in vacuum ,

$N_4 = (2.10 \pm 0.06) \times 10^{19} / \text{cm}^3$ for the sample annealed in the selenium atmosphere .

As can easily be seen, after irradiation the increase in the concentration of Cr²⁺ ions in the sample was about $10^{18} / \text{cm}^3$. The value of τ_0 obtained using Eq. (3) equals

$$\tau_0 = (1.00 \pm 0.003) \times 10^{-11} \text{ s} .$$

Since the Cr²⁺ ion has a Jahn-Teller (JT) active ground state, one should consider the possibility of a Jahn-Teller distortion. The real spinel structure is far from being

ideal. The chalcogenide spinels CdCr₂Se₄ used in the experiment have a number of selenium vacancies and other point defects (like Ga³⁺ ions). The interaction of such lattice imperfections with the Cr²⁺ ions, resulting in the removal of the orbital degeneracy of the ⁵E term, may also influence the magnetocrystalline anisotropy.

The contribution of random low-symmetry fields to the FMR linewidth can be written in the form¹²

$$\begin{aligned} \Delta H &= \Pi / 9ND^4 (2S)^6 \tanh(\omega/2T) g(2\Delta) \omega^{-2} (f + 3\Phi) I_1(t) \text{ for } T < T_0 , \\ \Delta H &= 2N \tanh(\omega/2T) [2f(3\Phi)^{-1/2} - 1] g^{-1}(2\Delta) I_2(t) \text{ for } T > T_0 , \end{aligned} \quad (5)$$

where $t = T/\Delta$, N is the concentration of JT centers, D is the one-ion anisotropy constant, S is the spin of the JT ion, ω is the energy of magnons, Δ is the dispersion of random low-symmetry fields, the functions f and Φ are defined in Ref. 12 and $I_1(t)$ and $I_2(t)$ are given by

$$\begin{aligned} I_1(t) &= 2 \int_0^\infty dy y^{3/2} \exp(-y^2) \sinh(2y/t) , \\ I_2(t) &= \int_0^\infty dy y^{1/2} \exp(-y^2) \sinh(y/t) \cosh^{-3}(y/t) . \end{aligned}$$

Figure 11(b) shows the fits of $\Delta H(T)$ obtained by taking into account the Jahn-Teller mechanism. By means of these fits one can calculate the dispersion of the low-symmetry fields Δ and the energy of magnons ω . We obtain

$$\Delta/k = 1.879 \pm 0.002 \text{ K} ,$$

$$\omega/k = 1622 \pm 2 \text{ K} .$$

It is worth noting that both the slow relaxation mechanism and the Jahn-Teller mechanism might equally well account for the experimental results obtained here.

V. CONCLUSIONS

We have observed the photomagnetic changes in the ferromagnetic resonance spectra of CdCr₂Se₄. As mentioned above, these changes cannot be attributed to the interaction between the light-induced Cr²⁺ centers and domain walls. The photoinduced changes in the intensity of the FMR signal and the asymmetrical FMR line shape might be caused by the skin effect. The photomagnetic changes in the resonance field, FMR linewidth, and magnetocrystalline anisotropy of CdCr₂Se₄ may be equally well attributed to two different mechanisms: the slow relaxation mechanism and the Jahn-Teller effect. The experimental results do not allow one to conclude which mechanism is effectively operating. Further experimental investigations are needed in order to solve this problem.

ACKNOWLEDGMENT

This research was supported by the State Committee for Scientific Research under Grant No. 2 0464 9101.

- ¹N. Menyuk, K. Dwight, R. J. Arndt, and A. Wold, *J. Appl. Phys.* **37**, 1387 (1966).
²H. I. Pinch and S. B. Berger, *J. Phys. Chem. Solids* **29**, 2091 (1968).
³W. Lems, P. J. Rijniere, and P. F. Bongers, *Phys. Rev. Lett.* **21**, 1643 (1968).
⁴S. G. Rudov and V. G. Veselago, *Solid State Phys.* **21**, 3250 (1979).
⁵E. Mosiniewicz-Szablewska and H. Szymczak, *J. Magn. Magn. Mater.* **104-107**, 986 (1992).
⁶I. W. Shepherd, *Solid State Commun.* **8**, 1835 (1970).
⁷J. B. Goodenough, *J. Phys. Chem. Solids* **30**, 261 (1969); C. Haas, *Crit. Rev. Solid. State Sci.* **1**, 47 (1970).
⁸J. M. Ferreira, M. D. Coutinho-Filho, S. M. Rezende, and P. Gibart, *J. Magn. Magn. Mater.* **31-34**, 672 (1983).

- ⁹V. I. Salyganov, Ju. P. Shilnikov, Ju. M. Jakovlev, V. L. Fedorov, M. A. Vinnik, and E. V. Rubalskaya, *Solid State Phys.* **16**, 3174 (1974).
¹⁰L. N. Novikov, L. L. Golik, T. G. Aminov, and V. A. Zhegalina, *Solid State Phys.* **22**, 3032 (1980).
¹¹A. G. Gurevich, V. I. Karpovich, E. V. Rubalskaya, A. I. Bairamov, B. L. Lapovok, and L. M. Emiryan, *Phys. Status Solidi B* **69**, 731 (1975); A. G. Gurevich, Ju. M. Jakovlev, V. I. Karpovich, A. N. Ageev, and E. V. Rubalskaya, *Phys. Lett.* **40A**, 69 (1972).
¹²M. A. Ivanov, B. Ja. Mitrofanov, and A. Ja. Fishman, *Solid State Phys.* **24**, 1047 (1982).
¹³T. Okamoto, K. Ametani, and T. Oka, *Jpn. J. Appl. Phys.* **13**, 187 (1974).
¹⁴A. M. Clogston, *Bell System Technol. J.* **34**, 739 (1955).